SPANDIDOS PUBLICATIONS EXPERIMENTAL AND THERAPEUTIC MEDICINE 13: 2651-2656, 2017

Degradation of Mg-6Zn alloy stents does not influence the healing of the common bile duct *in vivo*

YIGANG CHEN[1*], NIANFENG SUN[1*], JIE ZHANG[1], SHAOXIANG ZHANG[2], CHANGLI ZHAO[3] and JIAZENG XIA[1]

[1]Department of General Surgery, Wuxi Second Hospital, Nanjing Medical University, Wuxi, Jiangsu 214002; [2]Suzhou Origin Medical Technology Co., Ltd., Suzhou, Jiangsu 215513; [3]State Key Laboratory of Metal Matrix Composites, School of Materials Science and Engineering, Shanghai Jiao Tong University, Shanghai 200240, P.R. China

Received November 13, 2015; Accepted December 19, 2016

DOI: 10.3892/etm.2017.4363

Abstract. To investigate the effects of Mg-6Zn alloy on the healing of the common bile duct (CBD), Mg-6Zn alloy stents were implanted into the CBDs of rabbits. Stainless steel stents were transplanted into a second group of rabbits to serve as a control. Computed tomography (CT) scanning was performed and weight loss was recorded to evaluate the *in vivo* degradation process. Hematoxylin and eosin staining and immunohistochemical analyses were performed to determine the expressions of transforming growth factor (TGF)-β, vascular endothelial growth factor (VEGF) and basic fibroblast growth factor (bFGF) and evaluate CBD healing. The Mg-6Zn stents maintained ~82 and ~50% of the original length, and ~90 and ~43% of the original CT value at 1 and 2 weeks post-operatively, respectively. The residual weights of the Mg-6Zn stents were ~89, ~42 and ~9% of the original weights at 1, 2 and 3 weeks post-operatively, respectively. At 3 weeks post-surgery, the CBD was completely healed, with no wounds observed in the 3 groups. VEGF expression in the Mg-6Zn stent group was lower than that in the stainless steel stent group at 3 weeks post-surgery (P=0.002). No significant differences were observed between the mean expressions of the TGF-β1 and bFGF genes at 1 and 2 weeks post-surgery. The results of the present study suggest that degradation of the Mg-6Zn alloy may not affect healing of the CBD.

Correspondence to: Dr Jiazeng Xia, Department of General Surgery, Wuxi Second Hospital, Nanjing Medical University, 68 Zhongshan Road, Wuxi, Jiangsu 214002, P.R. China
E-mail: chyg7676@alumni.sjtu.edu.cn

Dr Changli Zhao, State Key Laboratory of Metal Matrix Composites, School of Materials Science and Engineering, Shanghai Jiao Tong University, 800 Dongchuan Road, Shanghai 200240, P.R. China
E-mail: 13506187399@139.com

*Contributed equally

Key words: biodegradable stent, Mg-6 Zn alloy, common bile duct, healing

Introduction

Healing is a complex process involving angiogenesis, new tissue formation and tissue remodeling (1). Transforming growth factor (TGF)-β, vascular endothelial growth factor (VEGF) and basic fibroblast growth factor (bFGF) are released at the wound site and are presumed to be necessary for healing (2). The material used in medical implants should ideally have good mechanical properties without affecting the tissue healing. Previous studies have demonstrated that the Mg-6Zn alloy exhibits excellent biocompatibility and good mechanical properties in the common bile duct (CBD) (3-5). However, the effects of Mg-6Zn degradation on the healing of the common bile duct have yet to be confirmed.

Due to their good biocompatibility and mechanical properties, Mg alloys have attracted more attention and been used in surgical implants (6,7). Immersion weight loss, hydrogen evolution and electrochemical measurements are typically used to assess Mg alloy corrosion rates (4). In the past decade, computed tomography (CT) technology has made great advances, and CT scanning may be used to measure the length and density of implanted metallic materials (8,9). It may therefore be suggested that CT scanning may be an effective method of examining the degradation of implanted metallic materials.

In the present study, stents were prepared from biodegradable Mg-6Zn alloy and implanted in the CBD of rabbits. CT scanning was performed to measure changes in length and density and compared with the results of previous corrosion experiments. Additionally, TGF-β, VEGF and bFGF expressions were evaluated via immunohistochemical analyses to investigate whether degradation of Mg-6Zn alloys had an effect on the healing of the CBD.

Materials and methods

Materials. The biodegradable Mg-6Zn alloy and stainless steel stents were donated by Suzhou Origin Material and Medical Technology Co., Ltd. (Jiangsu, China). The biodegradable Mg-6Zn alloy was prepared from high purity Mg (99.99%) and Zn (99.999%) as previously described (10). The composition of this alloy is displayed in Table I. The as-extruded Mg-6Zn rods were processed into tube-shaped samples with a luminal

Table I. Chemical compositions of Mg-6Zn alloy.

Material	Fe	Si	Ni	Cu	Al	Mn	Zn	Mg
Composition (weight %)	0.0038	0.0016	0.0005	0.0005	0.0085	0.0004	5.6210	94.3637

diameter of 1.0 mm, thickness of 0.1 mm and length of 5 mm for implantation into the CBDs of rabbits. Samples were cleaned ultrasonically with acetone and ethanol successively and sterilized with 29 kGy of 60 Co radiation prior to use in *in vivo* experiments.

Animals. All animal experiments were designed according to the Guidance Suggestions for the Care and Use of Laboratory Animals issued by the Ministry of Science and Technology of the People's Republic of China and approved by the Ethics Committee of the Wuxi Second Hospital, Nanjing Medical University. Animals were supplied by Sino-British Sippr/BK Lab Animal, Ltd., (Shanghai, China; license No: SCXK (hu) 2008-0016).

A total of 42 adult male New Zealand rabbits (mean age, 5±1 months) with a mean body weight of 1.3±0.4 kg were randomly and equally assigned to 2 groups (n=21); the research group and the control group. All rabbits were housed at 22-24˚C with a relative humidity of 50-60% and a 12 h light/dark cycle. Rabbits had free access to food and water, and were fasted for 12 h prior to and following surgery. In the research group, a tubular Mg-6Zn alloy stent was implanted into the CBD of each rabbit, whereas in the control group a stainless steel stent was implanted. Rabbits were anesthetized with ketamine hydrochloride (35 mg/kg; Jiangsu Hengrui Medicine Co., Ltd., Lianyungang, China). Rabbits were supplemented with a subcutaneous injection of 5% glucose and sodium chloride (Baxter International, Inc., Deerfield, IL, USA). A central venous catheterization set (CS-24301-E; Arrow International, Inc., Cleveland, OH, USA) was used to introduce the stents. Surgery was performed as described in a previous study by the present authors (11). In both the Mg-6Zn alloy and stainless steel stent groups, seven rabbits were sacrificed at 1, 2 and 3 weeks post-operatively.

CT scanning. CT scanning (Somatom Sensation 16; Siemens Healthcare GmbH, Erlangen, Germany) was used to observe the *in vivo* degradation process throughout the study. CT scanning was conducted immediately following surgery and 1-3 weeks postoperatively. The length (cm) and CT value (HU) of the Mg-6Zn alloy and stainless steel stent were measured according to the Digital Image and Communications in Medicine standard (12) and SIENET Sky software (SIENET Sky-VA50B; Siemens Healthineers; Siemens Healthcare GmbH).

Hematoxylin and eosin (H&E) and immunohistochemical analyses. Rabbits were sacrificed 1, 2 and 3 weeks postoperatively and their CBD tissue was harvested. Tissue samples of 2 cm^2 surrounding the implants were fixed for 24 h at room temperature in 10% buffered formaldehyde (Beyotime Institute of Biotechnology Institute of Biotechnology, Haimen, China) and subsequently cut to a thickness of 4 μm and mounted on glass slides. Histological slices were stained with H&E, tissue sections were deparaffinized in xylene and subsequently rehydrated in graded concentrations of ethyl alcohol (100, 95, and 75%) and water. The sections were then microwave-treated twice in citrate buffer (pH 6.0; Beyotime Institute of Biotechnology) at 99˚C for 6 min. Sections were placed in 3% H_2O_2 (Beyotime Institute of Biotechnology) for 10 min to inhibit endogenous peroxide activity, washed for 5 min three times with phosphate-buffered saline (PBS) and placed in normal mouse serum (1:5; cat. no. P0102; Beyotime Institute of Biotechnology) as a blocking antibody at room temperature for 10 min. Sections were treated with anti-TGF-β1 antibody (1:100; TB21; cat no. ab27969; Abcam, Cambridge, UK), anti-VEGF antibody (1:150; cat no. ab46154; Abcam) and anti-FGF basic antibody (1:150; cat no. ab16828; Abcam), incubated for 24 h at 4˚C and washed for 10 min three times with PBS. Sections were subsequently incubated for 30 min at room temperature with biotinylated anti-mouse/rabbit immunoglobulin (1:200; cat. no. A0216; Beyotime Institute of Biotechnology) was used as a secondary antibody and 3,3-diaminobenzidine tetrahydrochloride (0.05%; cat. no. ST033; Beyotime Institute of Biotechnology) was used as a chromogen. Cytoplasmic staining was evaluated as positive for TGF-β1, VEGF or bFGF. The sections were evaluated using a light microscope and a computer-assisted image analysis system (Motic Images 2000; version 1.3; Motic Incorporation, Ltd., Causeway Bay, Hong Kong). The expression of all apoptosis-associated proteins was determined via the integrated optical density (IOD) using Motic Fluo 1.0 software (Motic Incorporation, Ltd.).

Statistical analysis. Statistical analysis was performed with the SPSS 18.0 software package (SPSS Inc., Chicago, IL, USA). The experimental values were analyzed using paired-sample *t*-tests and all data are presented as the mean ± standard deviation. One-way analysis of variance analysis was performed to evaluate differences between groups. The Kruskal-Wallis test was used when equal variances were not assumed. $P<0.05$ was considered to indicate a statistically significant difference.

Results

Degradation of the Mg-6 Zn alloy stent in vivo. The degradation of the Mg-6Zn alloy stent was evaluated via CT scanning. A total of 42 adult New Zealand rabbits were included in the final analysis. All animals survived for the duration of the study and had stable body weights. The rabbits in each group grew normally and were able to freely carry out normal activities. No postoperative adverse effects, such as infection, pyrogenesis or effusion of bodily fluids were observed in any rabbits during the experimental period.

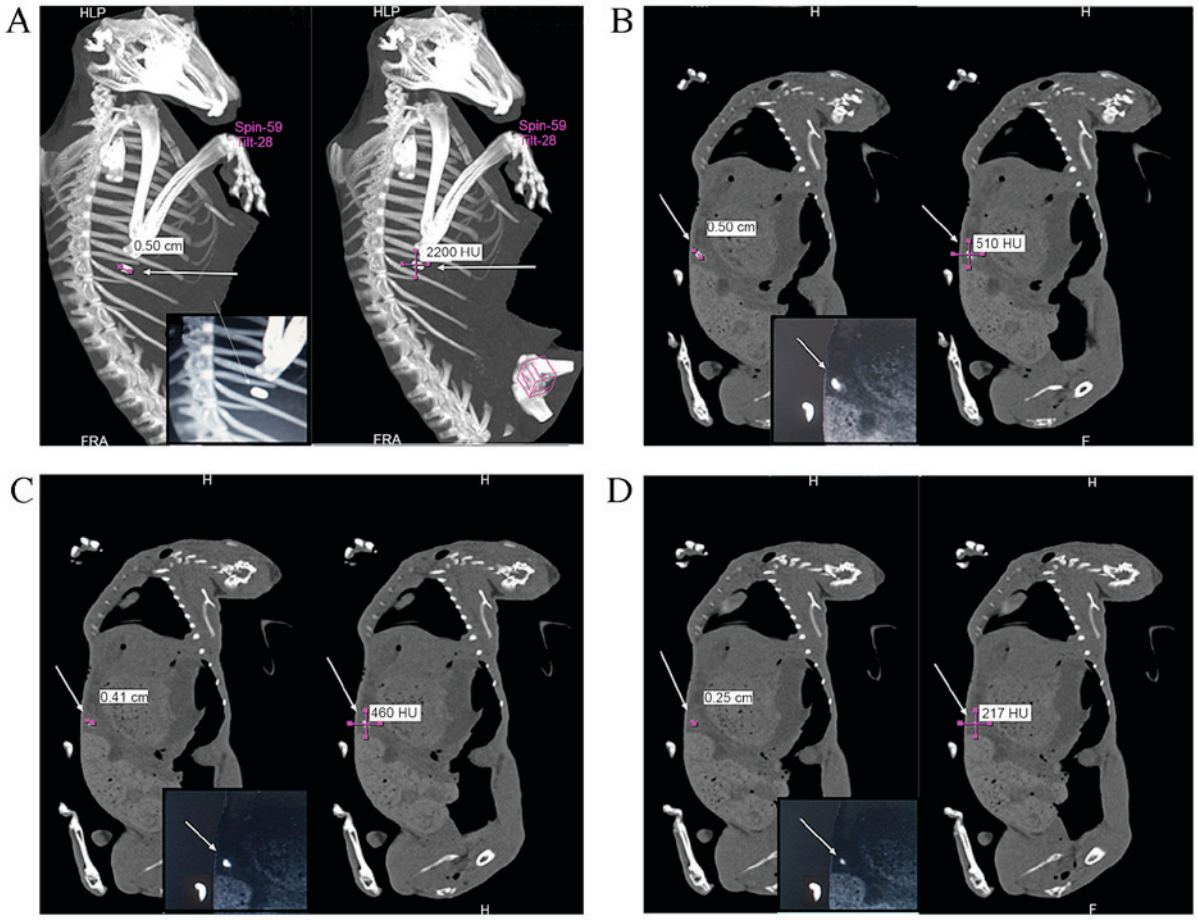

Figure 1. Representative pictures of CT scanning. (A) Length and CT value of the stainless steel stent and the partially magnified picture of the stainless steel stent. (B) Length and CT value of the Mg-6Zn stent on the day of operation and the partially magnified picture of the Mg-6 Zn stent on the day of operation. (C) Length and CT value of the Mg-6Zn stent 1 week post-surgery and the partially magnified picture of the Mg-6 Zn stent 1 week post-surgery. (D) Length and CT value of the Mg-6Zn stent 2 weeks post-surgery and the partially magnified picture of the Mg-6Zn stent 2 weeks post-surgery. Magnification, x1.5. CT, computed tomography.

Immediately following surgery, CT scanning confirmed that the biodegradable Mg-6Zn stents and non-degradable stainless steel stents were successfully implanted in the CBDs. The stainless steel stents were 0.50 cm in length with a CT value of 2,200 HU on the day of surgery (Fig. 1A), whereas the Mg-6Zn stents were 0.50 cm with a CT value of 510 HU (Fig. 1B). At 1 week post-surgery, the main structure of the Mg-6Zn stent was still able to be observed, and at 2 weeks post-surgery, approximately half of the Mg-6Zn stent remained. At 3 weeks post-surgery, the stent was difficult to observe on the CT scan.

At 1 and 2 weeks post-surgery, the length of the Mg-6Zn stent was 0.41±0.03 and 0.25±0.01 cm, respectively (Fig. 1C and D). The length of the Mg-6Zn stents decreased significantly by ~18 (P=0.007) and ~50% (P<0.001) at 1 and 2 weeks post-surgery, respectively, compared with the pre-implantation value (Fig. 2A). The CT values of the Mg-6Zn stents were 460±52 and 217±35 HU (Fig. 1C and D), a marked decrease of ~9.8% at 1 week and a significant decrease of ~57.5% (P<0.001) compared with the pre-implantation value at 2 weeks post-operatively (Fig. 2B). Stents were weighed immediately post-sacrifice at 1, 2 and 3 weeks post-surgery. The original weight of the Mg-6Zn stent was 2.5±0.21 mg and the remaining weight was approximately 89, 42 and 9% of the original at 1, 2 and 3 weeks post-surgery, respectively (Fig. 3), with the final weight being significantly lower than the original weight (P<0.001). These results indicate that Mg-6 Zn alloy stents were degraded by ~11, ~58 and ~91% at 1, 2 and 3 weeks post-surgery, respectively.

H&E and immunohistochemical evaluation in vivo. At 3 weeks post-surgery the CBD was completely healed, and no wound was observed in the 2 groups under direct vision (Fig. 4A). H&E staining revealed no marked cell swelling or infiltration of neutrophils or monocytes at 3 weeks post-surgery (Fig. 4B).

Figs. 5-7 demonstrate representative immunohistochemical pictures depicting the experiment on the TGF-β1, VEGF and bFGF genes in the peri-implant CBD tissues, and the statistical results of the immunohistochemical analysis. Based on the immunohistochemical IOD results, no significant differences were observed in expressions of TGF-β1, VEGF and bFGF genes over time for the Mg-6Zn alloy or stainless steel stent groups. Additionally, there was no significant difference in the expression of TGF-β1 and bFGF among the 3 groups at 3 weeks post-surgery. VEGF expression in the Mg-6Zn alloy stent group was lower than that in the stainless steel stent group at 3 weeks post-surgery (P=0.002).

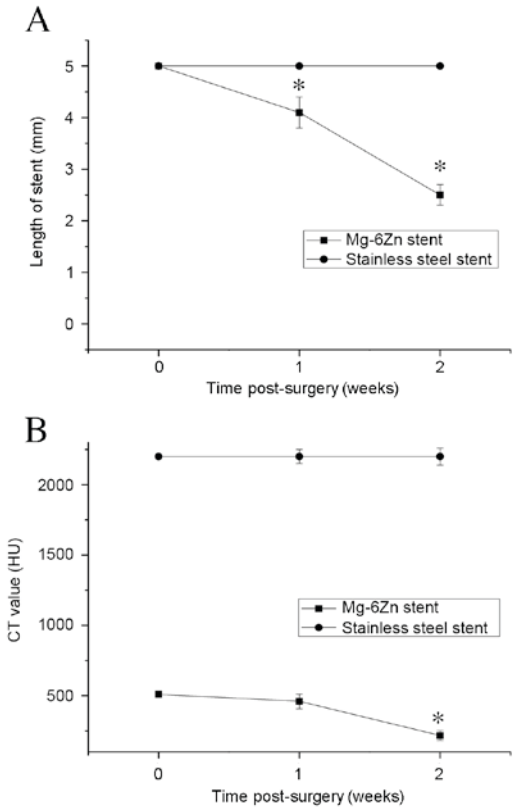

Figure 2. Results of the (A) length and (B) CT value of Mg-6Zn stent and stainless steel stent. *P<0.05 vs. day of surgery. CT, computed tomography.

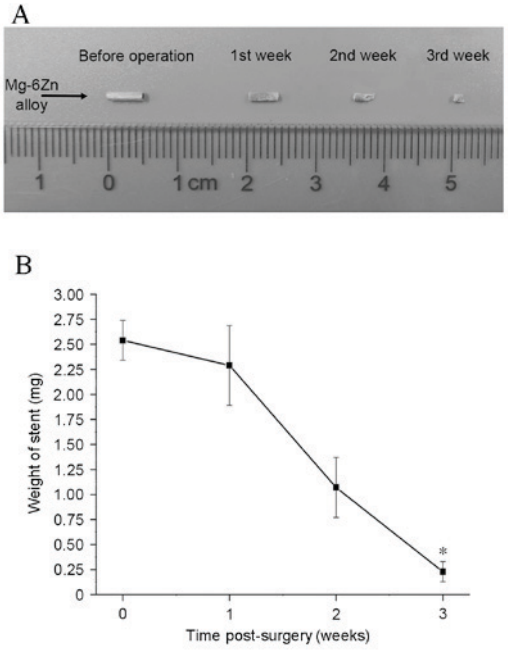

Figure 3. Results of the weight loss experiments *in vivo*. (A) Shape of the Mg-6Zn stent 1, 2 and 3 weeks post-surgery. (B) Weight evaluation of Mg-6Zn stent 1, 2 and 3 weeks post-surgery. *P<0.05 vs. prior to surgery.

Discussion

In the present study, Mg-6Zn alloy stents with a luminal diameter of 1.0 mm, thickness of 0.1 mm and length of 5 mm were implanted in New Zealand rabbits and were demonstrated via CT scanning to have degraded by ~82% at 1 week post-surgery, ~50% at 2 weeks post-surgery and almost completely degraded at 3 weeks post-surgery. Furthermore, stent density decreased by ~90.1% at 1 week post-surgery and ~42.1% at 2 weeks post-surgery. In the present study it was also demonstrated that implantation and subsequent degradation of Mg-6Zn alloy stents did not affect the expressions of TGF-β1 and bFGF whereas a decrease in VEGF expression was observed at 3 weeks post-surgery.

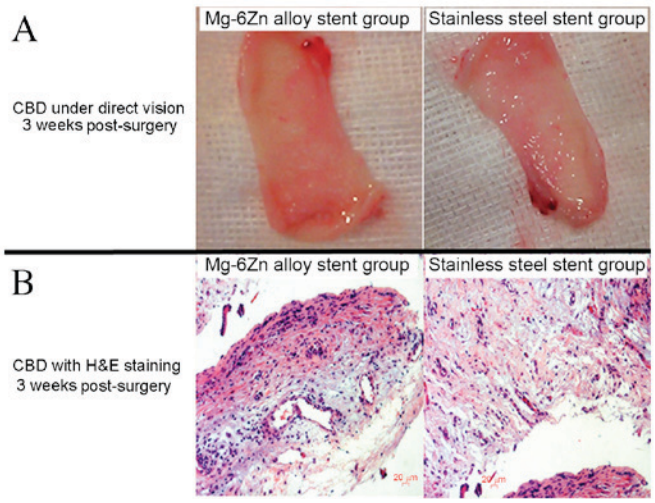

Figure 4. Representative pictures of tissue and H&E staining at 3 weeks post-surgery. (A) Representative pictures of tissue exam under direct vision. (B) Representative pictures of H&E stain analysis. CBD, common bile duct; H&E, hematoxylin and eosin.

There are many methods to detect the degradation of metal materials. Non-invasive CT scanning causes less damage to the experimental animal compared with surgery to remove the specimen *in vivo* (13). In the present study, Mg-6Zn alloy stents were removed from rabbits at 1, 2 and 3 weeks post-surgery and were demonstrated to have degraded to ~89, ~42 and ~9% of the original weight, respectively. The results of CT scanning (~82 and 50%, and almost completely degraded at 1, 2 and 3 weeks post-surgery, respectively) were similar to the weight loss results.

CT value represents tissue density (14), with a higher CT value indicating a greater density of implanted materials. The CT value of water is 0 HU, the minimum CT value of air is -2,000 HU and the maximum value of bone is 2,000 HU (15). Prior to implantation, the Mg-6Zn alloy stents had a mean CT value of 510 HU. At 2 and 3 weeks post-surgery, the CT value had decreased to 460 and 217 HU, respectively, indicating that the Mg-6Zn alloy stent had gradually degraded in the CBD. There are two possible explanations for this observation. First, when the Mg-6Zn alloy stent was implanted in the CBD, the surface of the sample was full of different-sized corrosion gaps and pits (4), resulting in a decreasing CT value. Second, the epithelial layer on the medical implants also contributed to the change in the CT value (16). In the CBD, the surface of the implanted stent easily becomes covered by bile duct endothelial cells and soft tissue (4). A greater duration of implantation leads to a greater amount of tissue covering a stent. The CT value of soft tissue is 20-70 HU,

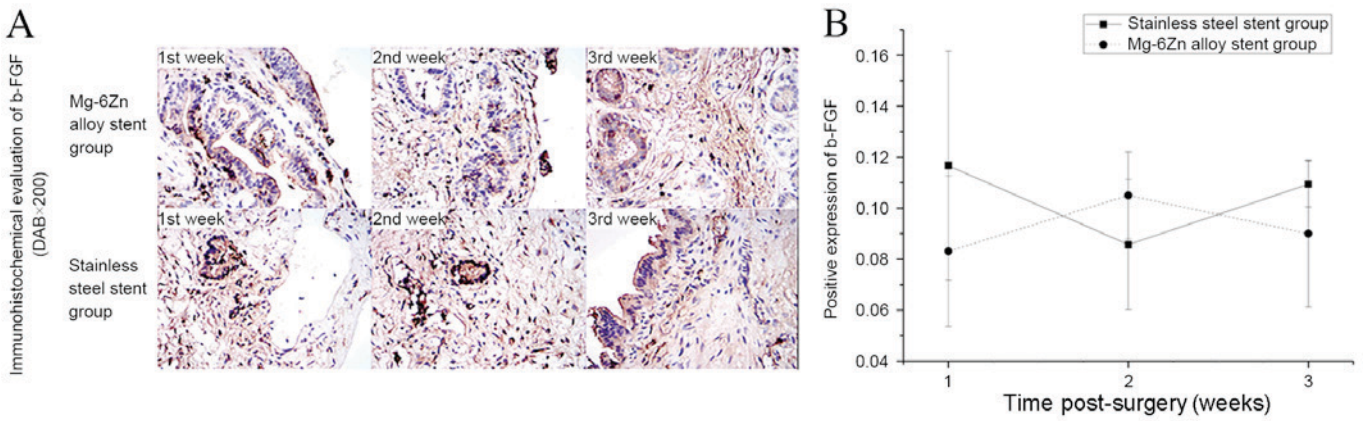

Figure 5. Immunohistochemical analysis of bFGF expression. (A) Representative immunohistochemical pictures of bFGF expression. (B) Statistical analysis of immunohistochemical analysis. bFGF, basic fibroblast growth factor; DAB, 3,3'-diaminobenzidine.

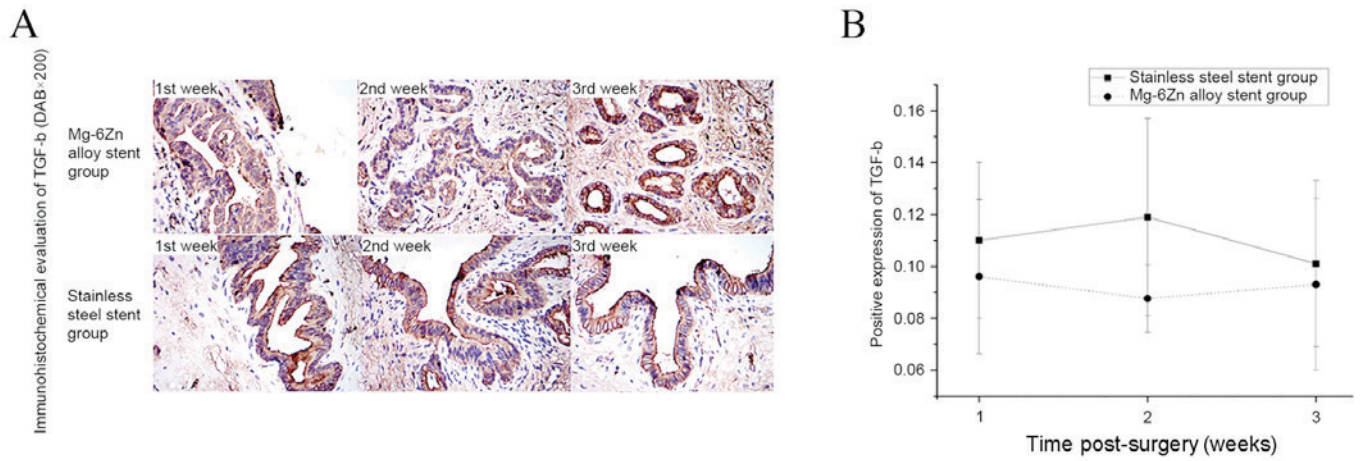

Figure 6. Immunohistochemical analysis of TGF-β expression. (A) Representative immunohistochemical pictures of TGF-β expression. (B) Statistical results of immunohistochemical analysis. TGF, transforming growth factor; DAB, 3,3'-diaminobenzidine.

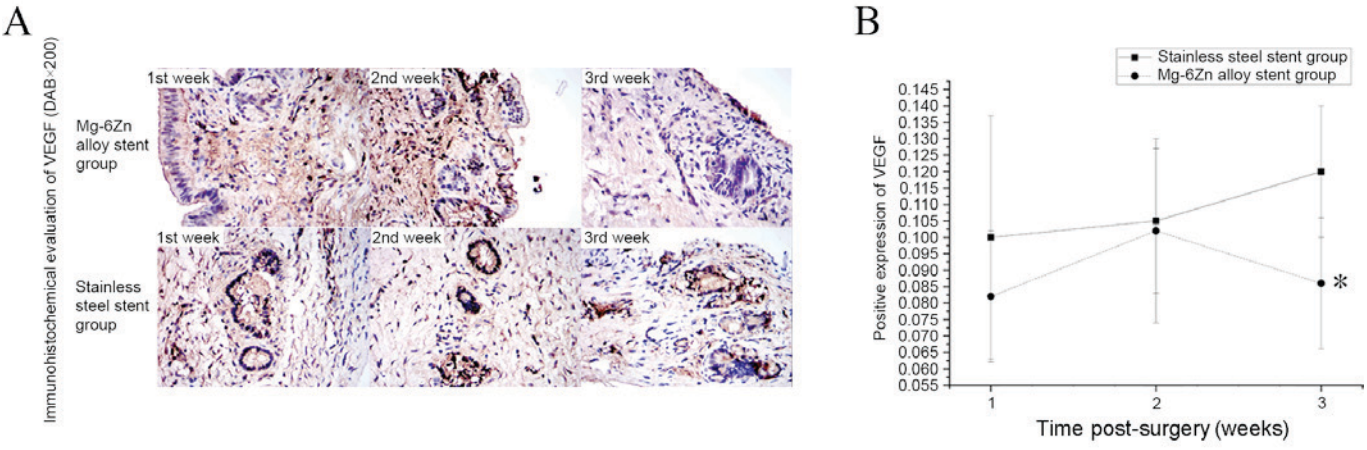

Figure 7. Immunohistochemical analysis of VEGF. (A) Representative immunohistochemical pictures of VEGF expression. (B) Statistical results of the immunohistochemical analysis. *P<0.05 vs. stainless steel stent group. VEGF, vascular endothelial growth factor; DAB, 3,3'-diaminobenzidine.

which may affect the measured CT value. In the present study, degradation data were different when the results of the length measurement and CT value assessment were compared. Based on this, it appears that CT scanning is able to demonstrate the trend of degradation, however the results are not accurate. The results of the present study suggest that that CT scanning may be used as an auxiliary method to assess the degradation of Mg alloys.

Growth factors such as TGF-β1 and bFGF are thought to be involved in wound healing (17,18). In the present study, the implantation of Mg-6Zn alloy and stainless steel stents did not affect wound healing or expression of the TGF-β1 and bFGF genes in the CBD, in accordance with a previous study; Yan *et al* (19) reported that the Mg-6Zn alloy has good biocompatibility properties and does not hinder the healing of the intestinal tract *in vivo*. However, the expression of another growth factor, VEGF, decreased 3 weeks post-surgery. VEGF serves key roles in ischemic wound healing (20) and the level of VEGF may reflect the degree of new vessel proliferation (21,22). Friction and chronic stimulation of the stent on the CBD wall decreased due to the degradation of Mg-6Zn, leading to a decrease in vascular proliferation resulting from friction. In the present study, VEGF levels in the non-degradable stainless steel stent group gradually increased, whereas it decreased in the biodegradable Mg-6Zn alloy stent group at 3 weeks post-surgery. This suggests that the change in VEGF expression was induced by the degradation behavior of the Mg-6Zn alloy in the CBD.

In the present study, Mg-6Zn alloy stents gradually degraded in the common bile ducts of rabbits. The lower levels of VEGF expression may be associated with decreasing stimulation resulting from the degradation of the Mg-6Zn alloy. The degradation behavior of the Mg-6Zn alloy does not appear to affect the expression of TGF-β/bFGF genes or wound healing in the CBD.

Acknowledgements

The present study was supported by Wuxi Hospital Administration Center Research Project (grant no. YGZXM1402) and the Nanjing Medical University Science and Technology Development Fund (grant no. 2014NJMUZD035).

References

1. Diegelmann RF and Evans MC: Wound healing: An overview of acute, fibrotic and delayed healing. Front Biosci 9: 283-289, 2004.
2. Ackermann M, Wolloscheck T, Wellmann A, Li VW, Li WW and Konerding MA: Priming with a combination of proangiogenic growth factors improves wound healing in normoglycemic mice. Int J Mol Med 27: 647-653, 2011.
3. Chen Y, Yan J, Zhao C, Zhang S, Yu S, Wang Z, Wang X, Zhang X and Zheng Q: In vitro and in vivo assessment of the biocompatibility of an Mg-6Z(n) alloy in the bile. J Mater Sci Mater Med 25: 471-480, 2014.
4. Chen Y, Yan J, Wang Z, Yu S, Wang X, Yuan Z, Zhang X, Zhao C and Zheng Q: In vitro and in vivo corrosion measurements of Mg-6Zn alloys in the bile. Mater Sci Eng C Mater Biol Appl 42: 116-123, 2014.
5. Chen Y, Yan J, Wang X, Yu S, Wang Z, Zhang X, Zhang S, Zheng Y, Zhao C and Zheng Q: In vivo and in vitro evaluation of effects of Mg-6Zn alloy on apoptosis of common bile duct epithelial cell. Biometals 27: 1217-1230, 2014.
6. Zhao J, Chen LJ, Yu K, Chen C, Dai YI, Qiao XY, Yan Y and Yu ZM: Effects of chitosan coating on biocompatibility of Mg-6%Zn-10%$Ca_3(PO_4)2$ implant. T Nonferr Metal Soc 25: 824-831, 2015.
7. Jia Z, Yang W, Zhang Z, Le Q and Cui J: Effect of ultrasonic melt treatment on degassing of Mg-6Zn-1Ca alloy. Res Dev 12, 2015.
8. Swain MV and Xue J: State of the art of Micro-CT applications in dental research. Int J Oral Sci 1: 177-188, 2009.
9. Krishna BV, Bose S and Bandyopadhyay A: Low stiffness porous Ti structures for load-bearing implants. Acta Biomater 3: 997-1006, 2007.
10. Zhang S, Zhang X, Zhao C, Li J, Song Y, Xie C, Tao H, Zhang Y, He Y, Jiang Y and Bian Y: Research on an Mg-Zn alloy as a degradable biomaterial. Acta Biomater 6: 626-640, 2010.
11. Chen Y, Yan J, Wang Z, Yu S, Yuan Z, Wang X, Zhang X and Zheng Q: Technique for the safe placement of a biodegradable stent into the common bile duct of rabbits. Exp Ther Med 6: 1101-1104, 2013.
12. Bidgood WD Jr, Horii SC, Prior FW and Van Syckle DE: Understanding and using DICOM, the data interchange standard for biomedical imaging. J Am Med Inform Assoc 4: 199-212, 1997.
13. Cressey D: Imaging animals for better research. http://www.nature.com/news/2011/110629/full/news.2011.391.html. Accessed March 4, 2015.
14. Cann CE: Quantitative CT for determination of bone mineral density: A review. Radiology 166: 509-522, 1988.
15. Borkan GA, Gerzof SG, Robbins AH, Hults DE, Silbert CK and Silbert JE: Assessment of abdominal fat content by computed tomography. Am J Clin Nutr 36: 172-177, 1982.
16. Yang DM, Jung DH, Kim H, Kang JH, Kim SH, Kim JH and Hwang HY: Retroperitoneal cystic masses: CT, clinical and pathologic findings and literature review. Radiographics 24: 1353-1365, 2004.
17. Okizaki S, Ito Y, Hosono K, Oba K, Ohkubo H, Amano H, Shichiri M and Majima M: Suppressed recruitment of alternatively activated macrophages reduces TGF-β1 and impairs wound healing in streptozotocin-induced diabetic mice. Biomed Pharmacother 70: 317-325, 2015.
18. Bennett NT and Schultz GS: Growth factors and wound healing: Biochemical properties of growth factors and their receptors. Am J Surg 165: 728-737, 1993.
19. Yan J, Chen Y, Yuan Q, Yu S, Qiu W, Yang C, Wang Z, Gong J, Ai K, Zheng Q, *et al*: Comparison of the effects of Mg-6Zn and titanium on intestinal tract in vivo. J Mater Sci Mater Med 24: 1515-1525, 2013.
20. Corral CJ, Siddiqui A, Wu L, Farrell CL, Lyons D and Mustoe TA: Vascular endothelial growth factor is more important than basic fibroblastic growth factor during ischemic wound healing. Arch surgery 134: 200-205, 1999.
21. Yancopoulos GD, Davis S, Gale NW, Rudge JS, Wiegand SJ and Holash J: Vascular-specific growth factors and blood vessel formation. Nature 407: 242-248, 2000.
22. Ferrara N: Vascular endothelial growth factor: Basic science and clinical progress. Endocr Rev 25: 581-611, 2004.